Nonaffine measures of particle displacements in sheared colloidal glasses

V. Chikkadi and P. Schall
van der Waals–Zeeman Institute, University of Amsterdam, Science Park 904, 1098XH Amsterdam, The Netherlands
(Received 28 December 2011; published 29 March 2012)

The nonaffine motion of particles is central to the relaxation and flow of glasses. It is usually assumed in plasticity theories that nonaffine rearrangements are localized and uncorrelated. Here we present evidence that this assumption may not hold. We investigate and compare systematically different measures of nonaffinity in a sheared colloidal glass by tracking the motion of the individual particles directly with confocal microscopy. We show that besides differences in the appearance and degree of localization of nonaffine displacements, the nature of their fluctuations is very similar. At intermediate times, all spatial correlation functions display robust power-law behavior, clearly demonstrating long-range correlations and critical behavior of the driven glass, in contrast to the assumptions of plasticity theories. We show that on long-time scales, correlations become finite and plasticity theories may apply.

DOI: 10.1103/PhysRevE.85.031402 PACS number(s): 82.70.Dd, 64.70.kj, 62.20.F−, 61.43.Fs

I. INTRODUCTION

The nature of displacement fluctuations in the flow of glasses and a wide range of amorphous materials is a topic of much current interest [1–10]. Unlike crystals, for which translationally invariant particles experience the same amount of local deformation under small, uniform applied stress, in amorphous materials, the varying environment of particles leads to strongly varying local deformation. As a result, particle displacements can no longer be described by a single affine transformation. In other words, in amorphous materials, the nonaffine displacements are of the same order as the relative affine displacements of the particles and the notion of affine displacements breaks down, giving rise to rich nonaffine physics [11–14]. Simulations have shown that treating the nonaffine displacements as small corrections to the affine displacements leads to inaccurate estimates of amorphous material properties [3,6,7]. Furthermore, rheological measurements on foams and emulsions have shown that these nonaffine displacements can lead to anomalous viscous loss [15]. Therefore, proper modeling of the mechanical properties of amorphous materials requires a good understanding of these nonaffine displacements. This is particularly important for plasticity theories that describe material flow based on constitutive equations. Identifying an appropriate order parameter to incorporate nonaffine contributions remains one of the grand challenges of such theories [4]. Insight into these nonaffine displacements can be obtained in steady-state flows. Recent quasistatic simulations have shown that in the athermal limit such flows are characterized by avalanches that span the entire system [1,2,5–8]. Such long-range-correlated displacements contrast with many plasticity theories that assume the nonaffine rearrangements to be localized and independent of each other [4,16]. Very recently, long-range correlations have been reported even for finite temperature and shear rate [17]. Experimental evidence, however, remains scarce and even in the quasistatic regime experiments and simulations may not agree [18]. One reason is that different definitions of nonaffinity have been used to measure the nonaffine displacements and a conclusive picture remains elusive [5,9].

In this paper we investigate systematically different measures of nonaffinity in a sheared colloidal glass. We image the motion of the individual particles directly with confocal microscopy and apply various definitions of nonaffinity to elucidate the nature of the nonaffine displacements. By comparing the fluctuations of different nonaffine measures, we show that, besides differences in the participation ratio, all definitions show very similar distribution functions with identical characteristics. We find that all distributions show consistent power-law decay and power-law correlation functions, clearly reflecting the criticality of the slowly driven glass.

II. EXPERIMENTAL SYSTEM

We prepare a colloidal glass by suspending sterically stabilized fluorescent polymethylmethacrylate particles at a volume fraction of $\phi \sim 0.60$ in a density and refractive index matching mixture of cycloheptyl bromide and cis-decalin. The particles have a diameter of $\sigma = 1.3\ \mu$m, with a polydisperity of 7% to prevent crystallization. The suspension is loaded in a cell between two parallel plates 3 mm in diameter, a distance of 65 μm apart. A schematic of the shear cell is shown in Fig. 1. A rod immersed in a reservoir of colloidal suspension is used to apply slow shear. The two parallel boundaries are coated with a layer of polydisperse particles to avoid boundary-induced crystallization. We use a piezoelectric translation stage to move the top plate to apply shear at a rate of $\dot{\gamma} = 1.5 \times 10^{-5}\ \mathrm{s}^{-1}$ with a maximum strain of 140%. Confocal microscopy is used to image the individual particles and to determine their positions in three dimensions with an accuracy of 0.03 μm in the horizontal and 0.05 μm in the vertical direction [19]. We tracked the motion of $\sim 2 \times 10^5$ particles during a 25-min time interval by acquiring image stacks every 60 s. All measurements presented here were made after the sample has been strained to 100%, well in the steady-state regime, as confirmed by independent rheological measurements.

 ©2012 American Physical Society

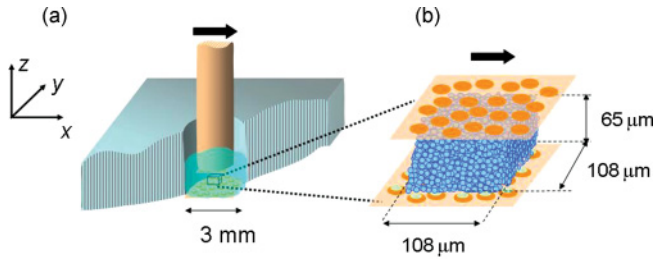

FIG. 1. (Color online) (a) Schematic showing the shear setup with the colloidal sample (cutaway) and the two opposing plates (center). (b) Enlarged section depicting the volume imaged with the confocal microscope.

III. NONAFFINE MEASURES OF PARTICLE DISPLACEMENTS

When a crystal is subject to small shear deformation, the particles exhibit affine motion; the local strain of the particles relative to their neighbors is the same and equal to the externally imposed strain. In an amorphous solid, however, the displacements are highly nonaffine; the local strain is heterogeneous. The nonaffine displacements are typically of the same order of magnitude as the relative affine displacements of neighboring particles and therefore cannot be considered as small corrections to affine deformation. Ignoring them, or treating them as a perturbation, yields highly inaccurate estimates for macroscopic material properties such as the elastic moduli [3,20]. In this paper we investigate various measures of nonaffinity in a sheared colloidal glass.

A. Deviations from the global deformation $\Delta\tilde{\mathbf{r}}$

The most widely used definition of nonaffine displacement is with respect to the global deformation [21], which can be expressed as

$$\Delta\tilde{\mathbf{r}}_i(t,\delta t) = \mathbf{r}_i(t) - \mathbf{r}_i(t-\delta t) - \dot{\gamma}\int_{t-\delta t}^{t} dt' z_i(t')\mathbf{e}_x. \quad (1)$$

Here i is the particle index, δt is the time interval over which the displacements are computed, $\dot{\gamma}$ is the shear rate, and $\mathbf{e}_x$ is the unit vector in the x (flow) direction. Equation (1) describes the deviation of the displacement of particle i from a linear displacement profile.

B. Deviations from locally affine motion D^2

A local measure of nonaffinity is achieved by mapping the motion of nearest-neighbor particles on an affine transformation. This is done by identifying the nearest neighbors of each particle as those separated by less than d_0, the first minimum of the pair-correlation function, and determining the best affine tensor $\mathbf{\Gamma}$ that transforms the nearest-neighbor vectors over the time interval δt. The best affine transformation $\mathbf{\Gamma}$ is determined by minimizing the quantity D^2, which is defined as the mean-square difference between the actual displacements of the neighboring particles relative to the central one and the relative displacements they would have if they were in a region of uniform deformation $\mathbf{\Gamma}$. That is, we define [4]

$$D^2(t,\delta t) = \sum_n \sum_i \Bigg(r_n^i(t) - r_0^i(t) - \sum_j (\delta_{ij} + \Gamma_{ij}) \times \left[r_n^j(t-\delta t) - r_0^j(t-\delta t) \right] \Bigg)^2, \quad (2)$$

where the indices i and j denote spatial coordinates; the index n runs over all the neighbors, $n = 0$ being the reference particle; and $r_n^i(t)$ is the ith component of the position of the nth particle at time t. We find the tensor Γ_{ij} that minimizes D^2 by calculating

$$X_{ij} = \sum_n \left[r_n^i(t) - r_0^i(t) \right] \left[r_n^j(t-\delta t) - r_0^j(t-\delta t) \right], \quad (3)$$

$$Y_{ij} = \sum_n \left[r_n^i(t-\delta t) - r_0^i(t-\delta t) \right] \left[r_n^j(t-\delta t) - r_0^j(t-\delta t) \right], \quad (4)$$

$$\Gamma_{ij} = \sum_k X_{ik} Y_{kj}^{-1} - \delta_{ij}. \quad (5)$$

The minimum value of $D^2(t,\delta t)$ is then the local deviation from an affine deformation or the nonaffine deformation during the time interval $[t-\delta t, t]$. This quantity has been reported to be an excellent metric of plasticity that detects local irreversible shear transformations [4,22].

C. Displacement fluctuations $\Delta\mathbf{r}'$

Another local measure of nonaffinity is based on the fluctuations of particle displacements with respect to a coarse-grained displacement field. Motivated by the ideas of classical mechanics and kinetic theory, Goldenberg *et al.* [5] defined fluctuations of the displacement and studied their correlations. We incorporate these ideas to define a coarse-grained displacement field, which is continuous, and a fluctuating part that is obtained by subtracting the continuous displacement field from the individual particle displacements. We define the coarse-grained displacement field as

$$\mathbf{U}(\mathbf{r},t;\delta t) = \frac{1}{N}\sum_{i=1}^{N} \Delta\mathbf{r}_i(t,\delta t)\Phi(\mathbf{r}_i(t-\delta t) - \mathbf{r}) \quad (6)$$

and the fluctuations as

$$\Delta\mathbf{r}'_i(t,\delta t) = \Delta\mathbf{r}_i(t,\delta t) - \mathbf{U}(\mathbf{r}_i,t;\delta t), \quad (7)$$

where i is the particle index, N is the number of particles in the system, and Φ is a coarse-graining function. Here we use the rectangular function

$$\Phi(\mathbf{R}) = H\left(R^2 - d_0^2\right), \quad (8)$$

where H is the Heaviside function and d_0 is the first minimum of the pair-correlation function. We refer the readers to Refs. [5,23] for a detailed discussion of the coarse-graining procedures used in simulations.

D. Nearest-neighbor loss N_{NN}

Nearest-neighbor loss has been used as a measure of irreversibility [21] and we include it here in the comparison of nonaffine motion. Generally, a local rearrangement can be considered irreversible if the particles involved in the rearrangements lose a certain number of their neighbors. A

few computer simulations of quiescent glasses have used the criterion of four or more neighbor losses for identifying irreversible zones [24,25]. We adopt this procedure to pinpoint irreversible rearrangements in our colloidal glass. We first find the neighbors of each particle at any instant of time using the method of Delaunay tessellation. Then, by comparing the neighbors of each particle at time t and $t - \delta t$, we identify the neighbors that are lost during the time interval δt and determine their number $N_{\rm NN}$.

E. Choice of δt

The nature of the nonaffine displacements will depend on the time interval δt used to determine them. For quiescent glasses, it is known that at short δt, one probes the oscillation of particles in the nearest-neighbor cages, while at very large δt, one probes the long-time diffusion out of these cages; at intermediate time scales, at which particles are arrested, one probes their collective rearrangement. An elegant way to study the influence of the probe time on the dynamics has been given in the framework of the dynamic susceptibility [26]. Here we follow a simpler route based on the probability distribution of displacements. For uncorrelated displacements, the probability distributions are Gaussian, while with increasing spatial correlation, increasing deviation from a Gaussian distribution is expected. The deviation from a Gaussian distribution is measured by the kurtosis

$$\kappa_4 = \left\{ \frac{1}{3N} \sum_{i=1}^{N} \left[\frac{\Delta\tilde{x}_i - \overline{\Delta\tilde{x}}}{\sigma} \right]^4 \right\} - 1, \qquad (9)$$

allowing us to estimate the degree of correlation as a function of probe time interval δt. In this paper we focus on the time scale of maximally correlated motion, i.e., the time interval that maximizes κ_4.

IV. RESULTS

The mean-square displacement of particles as a function of time is shown in Fig. 2(a). Red squares indicate the quiescent glass and blue circles indicate the sheared glass. We estimate the structural relaxation time of the quiescent glass $\tau \sim 2 \times 10^4$ s from the requirement $\langle \Delta r(\tau)^2 \rangle = (\sigma/2)^2$. When the shear is applied, this relaxation time shortens to $\tau_s \sim 4000$ s, clearly indicating the enhanced particle diffusion associated with the applied shear. To estimate the degree of correlation, we show the relative frequency of nonaffine displacements for two different time intervals in Fig. 2(b). The tails of these distributions differ significantly from a Gaussian distribution (dotted line). For quiescent glasses, such non-Gaussian behavior has been attributed to correlated dynamics. We assume here that the same interpretation holds for the sheared glass; we will see below that this is indeed the case. Apparently, the deviation from the Gaussian distribution is stronger for shorter-time intervals. We quantify this deviation by calculating the kurtosis κ_4, which we show as a function of time in the inset of Fig. 2(b). The kurtosis κ_4 exhibits a maximum at short times; on this time scale, we therefore expect maximum correlated motion and we will focus on this regime in the following.

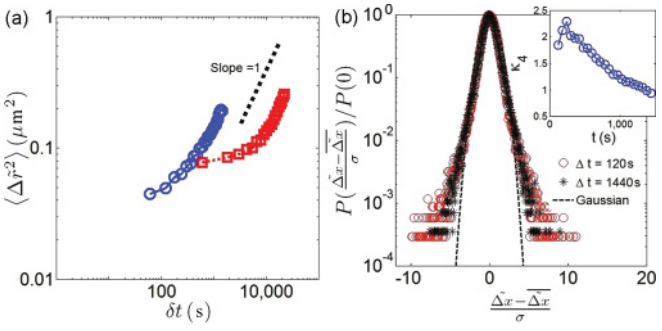

FIG. 2. (Color online) (a) Mean-square displacement of the quiescent [red squares (right)] and sheared glass [blue circles (left)]. Here we used $\langle \Delta\tilde{r}^2 \rangle$, the mean-square displacement around the mean global deformation [Eq. (1)]. (b) Normalized probability distribution of nonaffine displacements (x component of $\tilde{\Delta r}$) obtained at a shear rate of $\dot{\gamma} = 1.5 \times 10^{-5}$ s^{-1} and over two different time intervals. The black dashed line is a Gaussian distribution of zero mean and unit variance. The inset shows kurtosis κ_4 as a function of time.

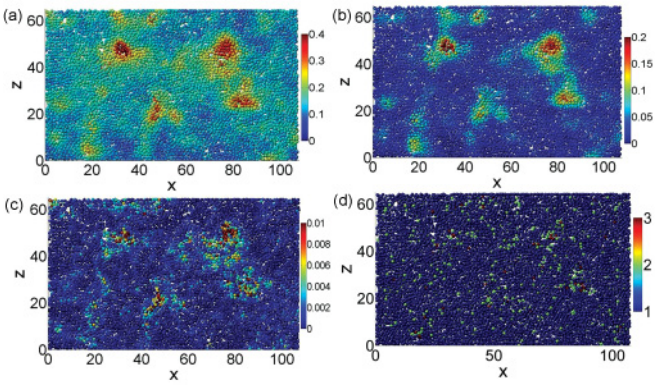

FIG. 3. (Color) Real-space renderings of the magnitude of nonaffine motion for various nonaffine measures: (a) deviation from the global deformation $\tilde{\Delta}r^2$, (b) deviation from local affine motion D^2, (c) fluctuations around a coarse-grained displacement field $\Delta r'^2$, and (d) number $N_{\rm NN}$ of neighbors lost. A time interval $\delta t = 120$ s was used.

Real-space distributions of nonaffine displacements for short-time intervals are shown in Figs. 3(a)–3(d). The panels show $\Delta\tilde{r}^2$, D_m^2, $\Delta r'^2$, and $N_{\rm NN}$, respectively, in a 5-μm-thick section of the glass parallel to the xz plane. The magnitude of nonaffine motion is represented with color: blue spheres indicate particles with small nonaffine motion, while red spheres indicate particles with large nonaffine components. Red zones in Figs. 3(a)–3(c) demarcate regions of highly nonaffine rearrangements; the particles in these regions have diffused more compared to the rest. These zones are the active zones of plastic deformation and have been referred to as shear transformation zones [4,9,16,22,27]. The degree of localization of the nonaffine displacements can be quantified by the participation ratio $p_A = (\sum_i A_i A_i)^2 / N \sum_i (A_i A_i)^2$, where A_i is the nonaffine displacement of particle i and N is the total number of particles. The participation ratio p_A is of the order unity when all the particle participate in the deformation and scales as $1/N$ for strongly localized deformation that is concentrated over a few particles in the system. For the distributions in Figs. 3(a)–3(c) we

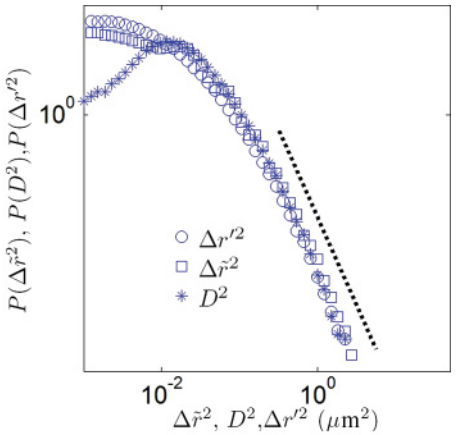

FIG. 4. (Color online) Probability distribution function of various nonaffine measures: $\tilde{\Delta}r^2$ (circles), D^2 (squares), and $\Delta r'^2$ (diamonds) obtained at a shear rate of $\dot{\gamma} = 1.5 \times 10^{-5}$ s^{-1}. The distributions are computed by taking an average over time intervals of $\delta t = 240$ s. The dashed line has a slope of -2.8.

obtain $p_{\Delta\tilde{r}} = 0.361 \pm 0.015$, $p_D = 0.413 \pm 0.02$, and $p_{\Delta r'} = 0.283 \pm 0.022$, showing that the nonaffine fluctuations of $\Delta r'$ are relatively more localized than those of D and $\Delta\tilde{r}$. Despite these differences, there is excellent overlap and all the definitions succeed in capturing the same zones of high activity. The red regions in Fig. 3(d) point to particles that have lost a maximum number of neighbors. This distribution appears much more scattered, but a careful comparison with Figs. 3(a)–3(c) shows that the neighbor loss is enhanced in regions where the nonaffine displacements are large, indicating that these nonaffine rearrangements are irreversible.

To obtain further insight into the nature of nonaffine fluctuations, we determine probability distribution functions (PDFs) and measure the spatial extent of fluctuations. We present PDFs of $\Delta\tilde{r}^2$, D^2, and $\Delta r'^2$ in Fig. 4. Interestingly, the tails of all PDFs display very similar power-law decay, associated with the same exponent $\beta = -2.8 \pm 0.2$. Incidentally, this exponent is very close to the value $\beta = 2.66$ that was reported in computer simulations of two-dimensional Lennard-Jones glasses [5]. Different characteristics, however, were observed in this work for the nonaffine displacements [Eq. (1)] and the displacement fluctuations [similar to Eq. (7)]. Both exhibited a power-law decay, however, with a different exponent. Our results show no such difference and we observe the same power-law distribution for all nonaffine measures within the error margin of our experiment. We note that the rearrangements studied here are irreversible, leading to plastic flow, while the ones studied in Ref. [5] are reversible and in the elastic regime, which may explain the difference.

The power-law distribution that we observe gives evidence of critical behavior of the driven glass. To elucidate this critical behavior, we measure how far the fluctuations of nonaffine displacements extend in space. We determine the normalized spatial correlation function

$$C_A(\delta r) = \frac{\langle A(r+\delta r)A(r)\rangle - \langle A(r)\rangle^2}{\langle A(r)^2\rangle - \langle A(r)\rangle^2}, \qquad (10)$$

where $A = D_m^2$, $\Delta\tilde{r}^2$, or $\Delta r'^2$ and δr is the distance between two particles. Here $\Delta\tilde{r}$ and $\Delta r'$ are the magnitudes of the vectors defined by Eqs. (1) and (7), respectively. The normalized spatial correlation function C_A correlates fluctuations of nonaffine displacements at two points separated by δr. Spatial correlation functions of D^2 (solid line), $\Delta\tilde{r}^2$ (dotted line), and $\Delta r'^2$ (dash-dotted line) are shown in Fig. 5. Remarkably, all these definitions display the same power-law decay up to $\delta r = 50\sigma$, the vertical system size, indicating that these fluctuations are long ranged, and there is no characteristic length scale associated with the nonaffine displacements. Furthermore, the different measures of nonaffinity are characterized by a unique exponent $\alpha = -1.2 \pm 0.1$. In contrast, the simulations of two-dimensional Lennard-Jones glasses [5] showed different spatial correlations for the nonaffine displacements [Eq. (1)] and the displacement fluctuations [similar to Eq. (7)]. The former were observed to be long ranged, while the latter appeared short ranged. We do not observe this difference in the plastic flow and our results demonstrate robust power-law decay for all definitions of nonaffinity. Such long-range correlation may originate from the glass elasticity: Shear transformations introduce long-range quadrupolar elastic strain fields [28] that couple to the external applied stress and to each other [29,30]. The resulting interactions can give rise to spatiotemporal correlation and to critical behavior of the flowing glass. Our results clearly show that this critical scaling is robust and independent of the specific definition of nonaffinity.

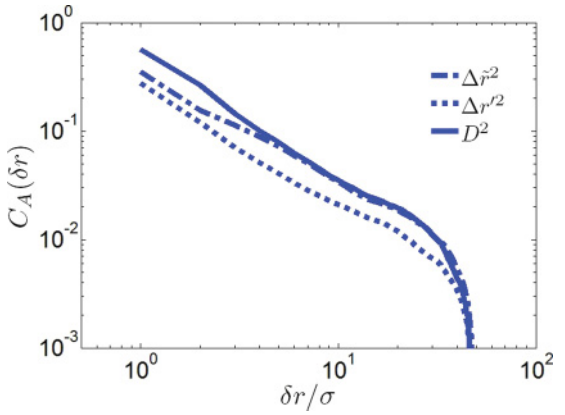

FIG. 5. (Color online) Angle-averaged spatial correlations of nonaffine displacements. Different line types represent the different definitions of nonaffinity. The solid line indicates D^2, the dash-dotted line indicates $\Delta r'$, and the dotted line indicates $\Delta\tilde{r}$.

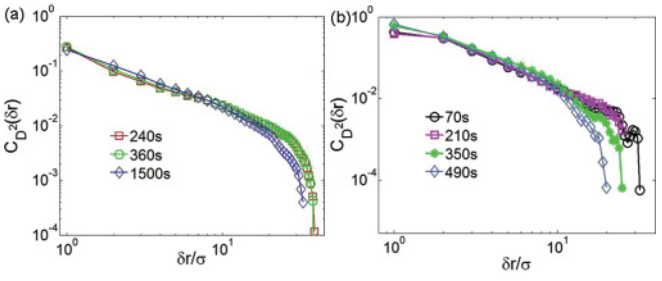

FIG. 6. (Color online) Angle-averaged spatial correlation functions of nonaffine displacements D^2 computed for various time intervals δt at a shear rate of (a) $\dot{\gamma} = 1.5 \times 10^{-5}$ s^{-1} and (b) $\dot{\gamma} = 2.2 \times 10^{-4}$ s^{-1}. Different line types are used to distinguish time intervals δt.

This scaling behavior depends, however, on the time scale used to compute the nonaffine displacements and the applied shear rate. To demonstrate this, we focus on the quantity D^2 [Eq. (2)] and show correlation functions for increasing time intervals in Fig. 6. Apparently, the correlation functions show a tendency to curve down earlier at longer-time intervals, suggesting a decreasing correlation length. While our limited time window does not allow us to clearly validate this point for the current strain rate of $1.5 \times 10^{-5}\ s^{-1}$ [Fig. 6(a)], we have performed shear experiments at a higher strain rate of $2.2 \times 10^{-4}\ s^{-1}$ [Fig. 6(b)] that show this trend more clearly. As the time interval grows, correlations become shorter ranged, indicating that nonaffine rearrangements become increasingly localized. While Fig. 6 shows only the nonaffine quantity D^2, all other nonaffine measures exhibit the same behavior. We conclude that on long-time scales, spatial correlations are lost and the rearrangements become increasingly localized and independent of each other.

V. CONCLUSION

We have investigated various nonaffine measures of the flow of amorphous materials using three-dimensional real-space measurements on colloidal glasses. We find that the fluctuations of all these nonaffine measures show very consistent characteristics. The persistent power-law probability distributions and power-law correlation functions that we observe clearly indicate critical behavior of the glass when slowly driven out of the arrested state. This long-range nature of the nonaffine displacements contrasts with mean-field theories of plasticity that assume rearrangements to be localized in space. While on long-time scales correlations are finite and these plasticity theories apply, at intermediate- and short-time scales correlations span the entire system, prohibiting the definition of a coarse-graining length scale on which constitutive equations of mean-field plasticity theories can be formulated, thereby calling for alternative concepts of such theories.

[1] C. E. Maloney and A. Lemaitre, Phys. Rev. Lett. **93**, 016001 (2004).
[2] C. E. Maloney and M. O. Robbins, J. Phys.: Condens. Matter **20**, 244128 (2008).
[3] J. L. Barrat, *Computer Simulations in Condensed Matter Systems: From Materials to Chemical Biology* (Springer, Berlin, 2006), Vol. 2, p. 287.
[4] M. L. Falk and J. S. Langer, Phys. Rev. E **57**, 7192 (1998); J. S. Langer, *ibid*. **77**, 021502 (2008).
[5] C. Goldenberg, A. Tanguy, and J. L. Barrat, Europhys. Lett. **80**, 16003 (2007).
[6] F. Leonforte, A. Tanguy, J. P. Wittmer, and J. L. Barrat, Phys. Rev. Lett. **97**, 055501 (2006).
[7] A. Tanguy, F. Leonforte, and J. L. Barrat, Eur. Phys. J. E **20**, 355 (2006).
[8] M. Tsamados, A. Tanguy, F. Leonforte, and J. L. Barrat, Euro. Phys. J. E **26**, 283 (2008).
[9] D. Chen, D. Semwogerere, J. Sato, V. Breedveld, and E. R. Weeks, Phys. Rev. E **81**, 011403 (2010).
[10] R. Besseling, E. R. Weeks, A. B. Schofield, and W. C. K. Poon, Phys. Rev. Lett. **99**, 028301 (2007).
[11] S. Alexander, Phys. Rep. **296**, 65 (1998).
[12] C. S. O'Hern, L. E. Silbert, A. J. Liu, and S. R. Nagel, Phys. Rev. E **68**, 011306 (2003).
[13] M. Wyart, S. R. Nagel, and T. A. Witten, Europhys. Lett. **72**, 486 (2005); M. Wyart, L. E. Silbert, S. R. Nagel, and T. A. Witten, Phys. Rev. E **72**, 051306 (2005).
[14] A. Ghosh, V. K. Chikkadi, P. Schall, J. Kurchan, and D. Bonn, Phys. Rev. Lett. **104**, 248305 (2010).
[15] A. J. Liu, S. Ramaswamy, T. G. Mason, H. Gang, and D. A. Weitz, Phys. Rev. Lett. **76**, 3017 (1996).
[16] F. Spaepen, Acta Metall. **25**, 407 (1977).
[17] J. Chattoraj, C. Caroli, and A. Lemaitre, Phys. Rev. E **84**, 011501 (2011); Phys. Rev. Lett. **105**, 266001 (2010); **103**, 065501 (2009).
[18] M. Twardos and M. Dennon, Phys. Rev. E **7171**, 061401 (2005).
[19] E. R. Weeks, J. Crocker, A. Levitt, A. B. Schofield, and D. A. Weitz, Science **287**, 627 (2000).
[20] A. Lemaitre and C. E. Maloney, J. Stat. Phys. **123**, 415 (2006).
[21] R. Yamamoto and A. Onuki, Phys. Rev. E **58**, 3515 (1998).
[22] P. Schall, D. A. Weitz, and F. Spaepen, Science **318**, 1895 (2007).
[23] I. Goldhirsch and C. Goldenberg, Eur. Phys. J. E **9**, 245 (2002).
[24] A. Widmer-Cooper, H. Perry, P. Harrowell, and D. R. Reichman, Nature Phys. **4**, 711 (2008).
[25] A. Widmer-Cooper, H. Perry, P. Harrowell, and D. R. Reichman, J. Chem. Phys. **131**, 194508 (2009).
[26] G. Biroli, O. Dauchot, and G. Marty, Phys. Rev. Lett. **95**, 265701 (2005); R. Candelier, O. Dauchot, and G. Biroli, *ibid*. **102**, 08801 (2009); F. Lechenault, O. Dauchot, G. Biroli, and J. P. Bouchaud, Europhys. Lett. **83**, 46003 (2008).
[27] A. Argon, Acta Metall. **27**, 47 (1979); A. S. Argon and Y. Kuo, Mater. Sci. Eng. **39**, 101 (1979).
[28] J. D. Eshelby, Proc. R. Soc. London. Ser. A **241**, 376 (1957).
[29] L. Bocquet, A. Colin, and A. Ajdari, Phys. Rev. Lett. **103**, 036001 (2009); G. Picard, A. Ajdari, F. Lequeux, and L. Bocquet, Phys. Rev. E **71**, 010501(R) (2005); Eur. Phys. J. E **15**, 371 (2004).
[30] V. Chikkadi, G. Wegdam, D. Bonn, B. Nienhuis, and P. Schall, Phys. Rev. Lett. **107**, 198303 (2011).